

Diagnosis of Static, Dynamic and Mixed Eccentricity in Line Start Permanent Magnet Synchronous Motor by Using FEM

Mohamed Moustafa Mahmoud Sedky

Abstract—In Line start permanent magnet synchronous motor, eccentricity is a common fault that can make it necessary to remove the motor from the production line. However, because the motor may be inaccessible, diagnosing the fault is not easy. This paper presents an FEM that identifies different models, static eccentricity, dynamic eccentricity, and mixed eccentricity, at no load and full load. The method overcomes the difficulty of applying FEMs to transient behavior. It simulates motor speed, torque and flux density distribution along the air gap for SE, DE, and ME. This paper represents the various effects of different eccentricity types on the transient performance.

Keywords—Line Start Permanent magnet, synchronous machine, Static Eccentricity, Dynamic Eccentricity, Mixed Eccentricity.

I. INTRODUCTION

High efficiency, improved power factor and enhanced torque density of line-start permanent magnet synchronous (LSPMSM) motors make them superior alternative to induction motors in many constant speed applications such as fans, pumps and compressors, comprising a considerable portion of the total electric motors applications. In industries and academic world, LSPMSM have received more attention in the last years [1]-[21]. A new requirement can be achieved by the use of it. Due to its high efficiency, high power factor, and its ability to self-start from regular fixed frequency supply, it became competitor to the squirrel cage induction motor. [4]-[7]. The functioning of the LSPMSM is characterized by two operation modes: The synchronous operation mode at steady state and the asynchronous operation mode at starting and transient [18]. The synchronizing process has been studied and the steady-state characteristics are measured for different values of the output power [1],[3],[11].

Eccentricity faults are among common types of faults in LSPMSM, they have effects on magnetic behavior of the motor. Damage to the mechanical elements of the motor such as bearing, and gear box is considered as a sort of the mechanical faults. About (50% to 60%) is the probability of these types of faults. Bearing fault about (40%-50 %) and eccentricity is about 60 % [22]-[24].

Existing of no uniform air gap between stator and rotor is a result of eccentricity, where there are Static Eccentricity (SE), Dynamic Eccentricity (DE), and Mixed Eccentricity (ME). In static eccentricity (SE), the rotational axis of the rotor

coincides with the symmetrical axis, but it displaces from the stator symmetrical axis. In dynamic eccentricity (DE), the stator symmetrical axis coincides with the rotor rotational axis, but the rotor symmetrical axis displaces. The static and dynamic eccentricities tend to coexist and in reality mixed eccentricity must be considered. In this case, the center of rotor, the center of stator, and the center of rotation are displaced with respect to each other. In the three cases air gap distribution is no uniform around the rotor and also time variant. Fig. 1 shows the cross sections of the LSPMSM with normal healthy machine and different types of eccentricities.

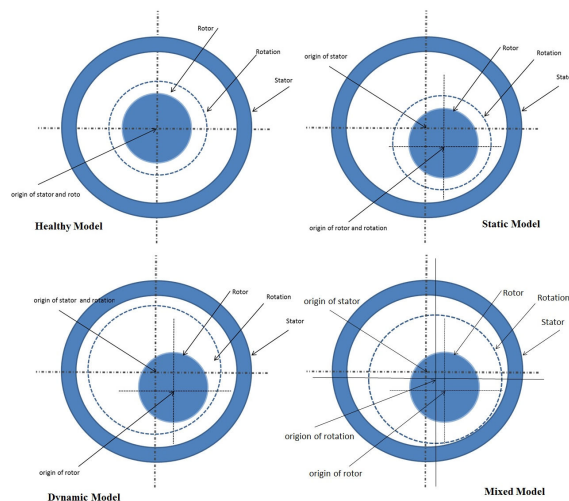


Fig. 1 LSPMSM with different eccentricities

II. FEM MODEL

Maxwell FE software is used to create the transient model of the machine. Where, in Fig. 2, it shows the 2D cross section FEM of the studied LSPMSM. The example of LSPMSM is 550 w, 4poles, $V=220$ volt, 3 phase, Y connection, 1500 RPM. It is main design data and the finite element 2D model in Table I and Fig.2. Where, the time-dependent magnetic equations for Maxwell FE software are used.

A. Static Eccentricity (SE)

Due to the symmetrical in the machine, the lower half eccentricity is studied only for SE. Fig.3 shows the positions of different cases of SE, while Table II shows the coordination of different cases of SE. where we have two regions of static

eccentricity, inner region for S1 to S5, and outer region for S6 to S10.

B. Dynamic Eccentricity (DE)

In dynamic eccentricity, different models are studied, where the rotor origin is changed each time. Where, we have 2 regions of origin location. Inner region is D1 to D4 and outer region is D5 to D8. As shown in Fig. 4 and the coordinates are in Table III.

C. Mixed Eccentricity (ME)

In dynamic eccentricity, different models are studied, and in mixed type, it is mixed between SE and DE. Where, the most effective cases in SE mixed with the most effective cases in DE to create the ME. Fig 5 and the coordinates are in Table IV. Where, we have 2 regions of origin. Inner region is M1 to M4, and outer region is M5 to M8.

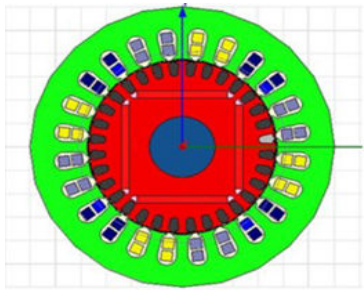


Fig. 2 2D Finite element model

TABLE I
LSPMSM DESIGN PARAMETERS

Design parameter	Value
Number of stator/rotor slots	24/20
Outer diameter of stator	120 mm
Inner diameter of stator	75 mm
Air gap length	1 mm
Axial Length of stator core	65 mm
Thickness of magnet	3 mm
Magnet material	NdFeB30
Stator resistance	10.06 Ω
Stator leakage inductance	0.00350831 H

TABLE II
THE COORDINATES OF DIFFERENT SE MODELS

Models of SE	Origin of rotor and rotation (mm)
S1	(0.2,0)
S2	(0.1,-0.1)
S3	(0,-0.2)
S4	(-0.1,-0.1)
S5	(-0.2,0)
S6	(0.4,0)
S7	(0.3,-0.3)
S8	(0,-0.4)
S9	(-0.3,-0.3)
S10	(-0.4,0)

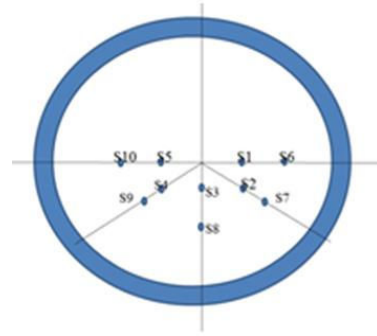


Fig. 3 Positions of different cases of SE

TABLE III
THE COORDINATES OF DIFFERENT DE MODELS

Model of DE	Rotor Origin (mm)
D1	(0.2,0.2)
D2	(0.2,-0.2)
D3	(-0.2,-0.2)
D4	(-0.2,0.2)
D5	(0.3,0.3)
D6	(0.3,-0.3)
D7	(-0.3,-0.3)
D8	(-0.3,0.3)

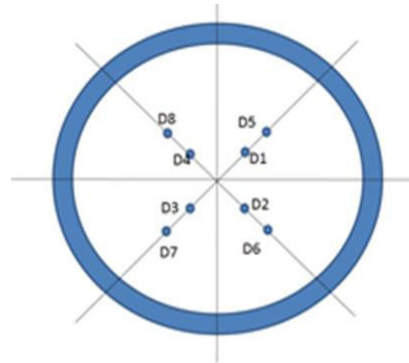


Fig. 4 Positions of different cases of DE

TABLE IV
THE COORDINATES OF DIFFERENT ME MODELS

Model of ME	Rotor origin	Rotation origin (mm)
M1	D1	(-0.1,0)
M2	D2	(-0.1,0.1)
M3	D3	(0.2,0)
M4	D4	(0.2,0)
M5	D5	(-0.2,0)
M6	D6	(-0.2,0.2)
M7	D7	(0.2,0)
M8	D8	(0.1,-0.1)

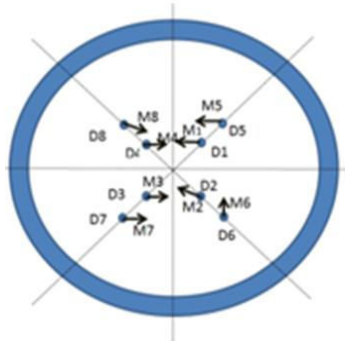


Fig. 5 Positions of different cases of ME

III. NO LOAD TEST

The no load performance is tested by applying 3 phase supply, 50 Hz, Y connected, with $TL=0.0$, and for healthy machine and non-healthy machine for all cases, SE, DE, and ME.

A. No Load Speed

For a speed, the no load static eccentricity (NLSE) has no big effect on the speed, for both over shooting and settling time, as shown in Figs. 6 and 7.

While for no load dynamic eccentricity (NLDE) in Figs.8 and9, it has big effect on the transient over shoot speed, and the settling time. It is increased from 100 ms to 200 msec. The worst case is D8 as shown in Fig.9.

For no load mixed eccentricity (NLME), as shown in Figs. 10 and11, the settling time has no change, while the only effect is shown in the transit over shooting speed, where the inner and outer region of NLME cases have effect on the transient over shooting only.

B. No Load Flux Density

For studying the flux density distribution over the contour on the middle of the air gap, as shown in Figs.12 to15, it is shown that, the inner region for NLSE has slightly effect on the flux density distribution, while the outer region of NLSE has big effect on the flux density distribution, where the air gap reluctance is not uniformly and the flux density is not uniformly distributed, as shown in Figs.12 and13.

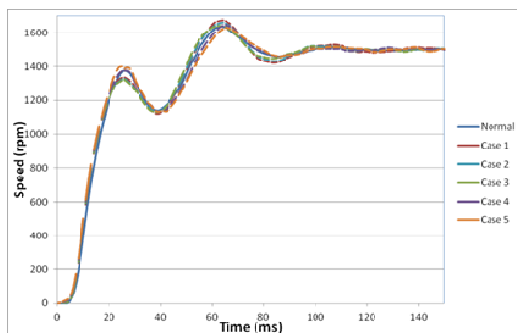


Fig. 6 No load speed for SE (the inner group)

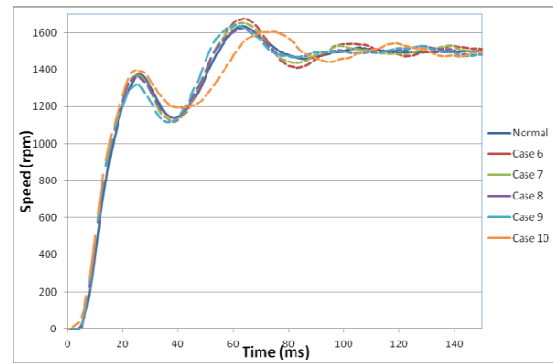


Fig. 7 No load speed for SE (the outer group)

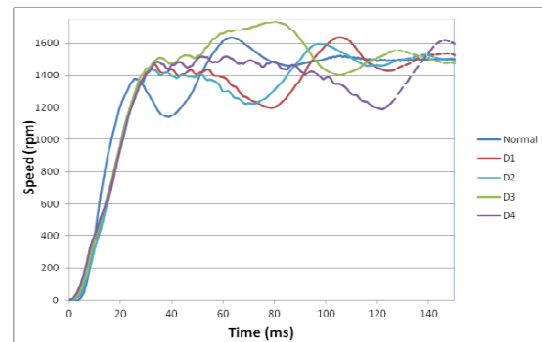


Fig. 8 No load speed for DE (the inner group)

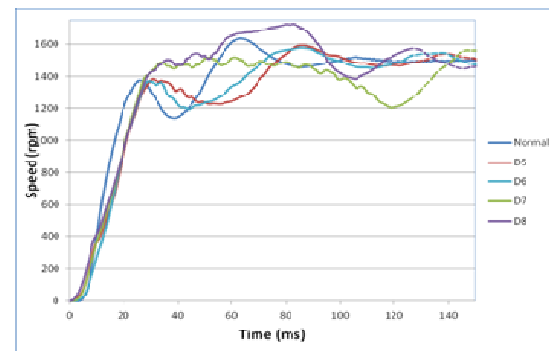


Fig. 9 No load speed for DE (the outer group)

For NLDE, the outer region has a big effect in distortion the flux density distribution, as shown in Fig.14. While for NLME, because it is combination from NLSE and NLDE.

For NLME, the flux density distortion is less than the NLDE. Analytical analysis of flux density effect for all the types is shown in Tables V-VII. For NLSE average Flux density is changing from -0.2% to 23% for case 8. And for dynamic, it has great effect as shown in Table VI, where it is changing from 16% to 36%. As found in the speed response, the NLME has less effect than NLDE, and higher than NLSE. Where, the average flux density is changing from 8.5% to nearly 19.7%. This is because the dynamic eccentricity effect is reduced by the static eccentricity effect.

For No load torque, three different cases are studied together, which are S8, D8, and M8 from the outer region.

Static eccentricity has no visible effect on the transient torque, while dynamic and mixed eccentricity has more distortions on the torque performance, as shown in Fig 16.

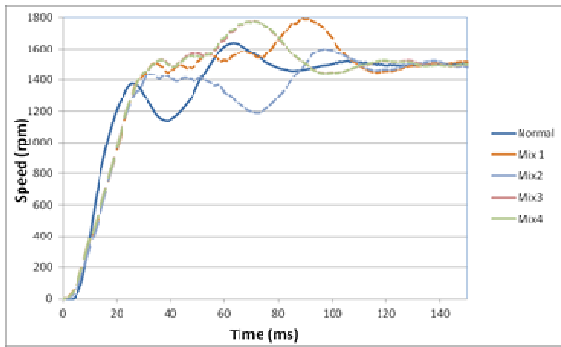


Fig. 10 No load speed for ME (the inner group)

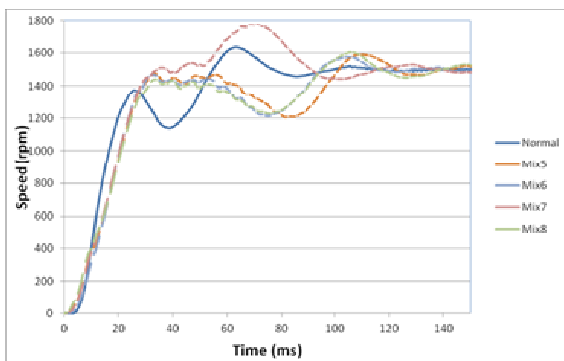


Fig. 11 No load speed for ME (the outer group) no load torque

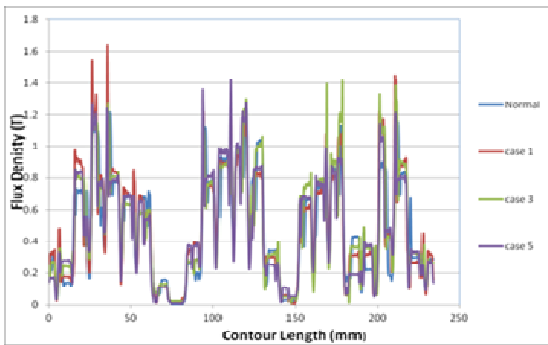


Fig. 12 Flux density distribution inside the air gap for NLSE (inner region)

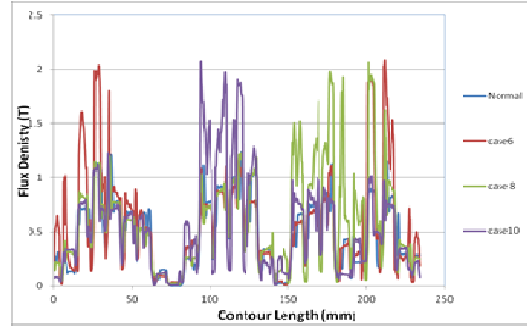


Fig. 13 Flux density distribution inside the air gap for NLSE (outer region)

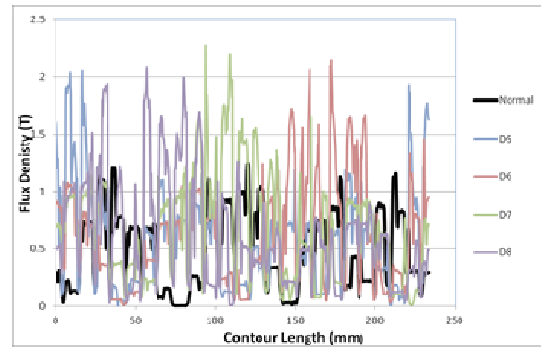


Fig. 14 Flux density distribution inside the air gap for NLDE (outer region)

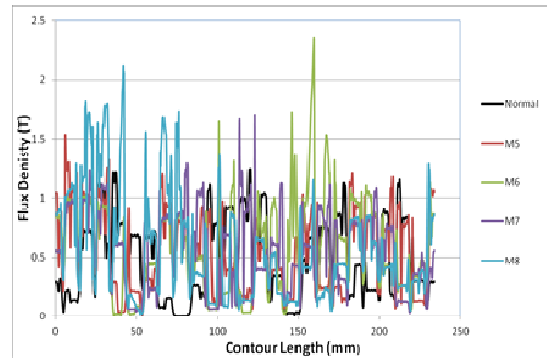


Fig. 15 Flux density distribution inside the air gap for NLME (outer region)

IV. LOAD TEST

Load analysis is studied under different cases for eccentricities, which are S8, D8, and M8, which considered the worst case of eccentricity as proofed from the no load analysis. Table VIII shows the percentage increase of speed with different types of eccentricities, where SE has nearly no effect of the speed and the settling time. While DE and ME has damping effect on the max over shoot speed, where it is reduced by 14.5 % in DE and 20.8 % in ME. That means the load has damping effect on the DE and ME. Fig. 17 shows the load performance for the three different types of eccentricities comparing with the normal one. DE and ME have effect on the starting torque, which is reduced from 15 Nm to nearly 9 Nm,

where SE has no effect on the torque performance. Also DE and ME have more repels on the steady state torque, which causes noise. The Rotor position at 60 msec is in Table IX. For normal and static case, the position is nearly the same, while in DE and ME there is delay in position.

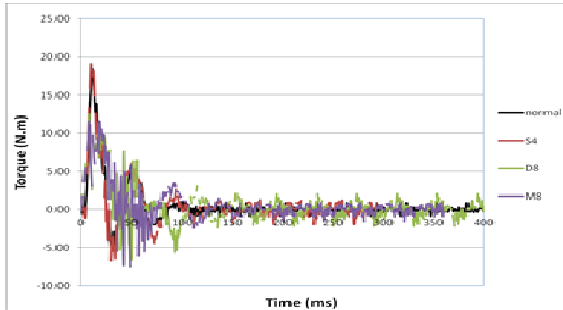


Fig. 16 No load torque in different cases

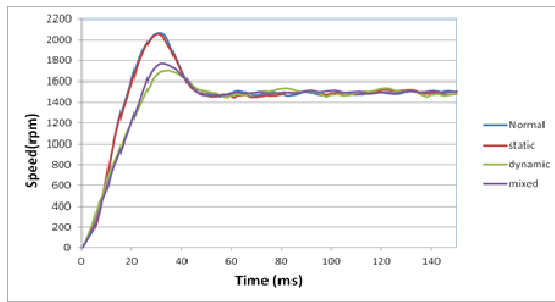


Fig. 17 Load speed at different eccentricities

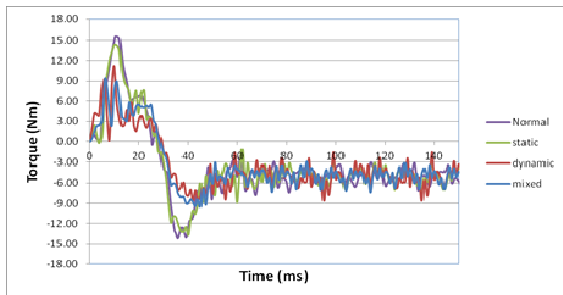


Fig. 18 Load torque at different eccentricities

TABLE V
FLUX DENSITY ANALYSIS OVER THE AIR GAP FOR NLSE

Normal average density is 0.4853 T, and max flux density is 1.21T			
Model	Average flux density(T)	Max (T)	%
Case 1	0.492281	1.64	1.43471044
Case3	0.503106	1.41	3.66507373
Case5	0.484304	1.418	-0.20904102
Case8	0.561066	2	16.0464670
Case9	0.594636	2	22.9634617
Case10	0.532368	2	10.133143

TABLE VI
FLUX DENSITY ANALYSIS OVER THE AIR GAP FOR NLDE

Model	Average flux density (T)	Max (T)	%
D5	0.5631738	2.1	16.04200236
D6	0.6070828	2.1	25.08943737
D7	0.6607360	2.25	36.14469861
D8	0.613965	2.05	26.50763581

TABLE VII
FLUX DENSITY ANALYSIS OVER THE AIR GAP FOR NLME

Model	Average flux density (T)	Max(T)	%
M5	0.52699607	1.53	8.587562047
M6	0.581241813	2.3	19.76489961
M7	0.553121528	1.7	13.9707136
M8	0.565532364	2	16.52796693

TABLE VIII
PERCENTAGE INCREASE IN OVER SHOOT SPEED

Case	Overshoot (rpm)	%
Normal	2055	
Static	2050	-0.25
Dynamic	1758	-14.5
Mixed	1629	-20.8

TABLE IX
ROTOR SPEED AND POSITION AT 60 MSEC

Type	Normal	SE	DE	ME
N (rpm)	1493	1459	1471	1486
θ (deg)	498	493	444	444

V. CONCLUSION

A diagnosis of the eccentricity of LSPMSM by using FE, is very successful in analysis and observes the flux density distribution and transient performance. By using FE model, it is very sensible to simulate the three different types of eccentricity with the non-linearity of the magnetic model, which are, SE, DE, and ME. Where, it is very difficult to test them in practical. FEM concluded that, the outer region of SE (S6 to S10) has sensible effect than the inner region of SE (S1 to S5). DE has a big effect on the speed over shooting, settling time, and the flux density distribution. ME effect lies between SE, and DE effects. In load condition, SE has no effect, while DE is still having the main dominate effect. Load effect has a damping effect on the eccentricity, which reduces the effect of Eccentricity to be less than the no load effect.

REFERENCES

- [1] F. Libert, J. Soulard, and J. Engstrom, "Design of a 4-pole line start permanent magnet synchronous motor," Proc. ICEM 2002, Brugge, Belgium, Aug. 2002.
- [2] J. Soulard and H.P. Nee, "Study of the synchronization of line-start permanent magnet synchronous motors," Proc. of 2000 IEEE Ind. Appl. Conf., Roma, 8-12 Oct. 2000, vol. 1, pp. 424-431.
- [3] K. Kurihara and A. Rahman, "High-efficiency linestart interior permanent-magnet synchronous motors," IEEE Trans. Ind. Appl., vol. 40, no. 3, May/Jun. 2004, pp. 789-796.
- [4] E. Peralta-Sanchez and A.C. Smith, "Line-start permanent-magnet machines using a canned rotor," Proc. IEMDC 2007, 3-5 May 2007, vol. 2, pp. 1084-1089.
- [5] J. Salo, T. Heikkilä, J. Pyrhonen, "New low-speed high-torque permanent magnet synchronous machine with buried magnets," Proc. ICEM 2000, 28-30 August, 2000, Espoo, Finland, vol. 2, pp. 1246-1250.

- [6] A. Abbas, H.A. Yousef, O.A. Sebakhy, "FEPParameters Sensitivity Analysis of an Industrial LSIInterior PM Synchronous Motor," IEEE Power and Energy Society General Meeting – Conversion andDelivery of Electrical Energy in the 21st Century, 20-24 July 2008 pp.1-6.
- [7] T. Ding, N. Takorabet, F.M. Sargos, and X. Wang, "Design and Analysis of Different Line-Start PMSynchronous Motors for Oil-Pump Applications," IEEE Trans. Magnetics, Vol. 45, No. 3, March 2009, pp. 1816-1819.
- [8] W.H. Kim, K.C. Kim, S.J. Kim, et al., "A Study on the Optimal Rotor Design of LSPM Considering the Starting Torque and Efficiency," IEEE Trans. Magnetics, Vol. 45, No. 3, March 2009, pp. 1808- 1811.
- [9] D. Rodger, H.C. Lai, R.J. Hill-Cottingham, P.C. Coles and F. Robinson, "A new high efficiency line start motor with high starting torque," Proc. Int. Conf. PEMD 2006, 4-6 April 2006, pp. 551-555.
- [10] L. Weili, Z. Xiaochen, C. Shukang, C. Junci, "Study of Solid Rotor Line-Start PMSM Operating Performance," Proc. ICEMS 2008, 17-20 Oct. 2008, pp.373-378.
- [11] G. Yang, J. Ma, J. and Y. Wang, "Optimal Design and Experimental Verification of a Line-Start Permanent Magnet Synchronous Motor," Proc. ICEMS 2008, 17-20 Oct. 2008, pp.:3232 – 3236.
- [12] I. Tsuboi, I. Hirotsuka, T. Takegami, and M. Nakamura, "Basic Concept of an Analytical Calculation Method and Some Test Results for Determination of Constant of Line Start Permanent Magnet Motor," Proc. ICEMS 2008, 17-20 Oct. 2008, pp. 3108-3111
- [13] M. Comanescu, A. Keyham, and Min Dai, "Design and analysis of 42-V permanent-magnet generator for automotive applications," IEEE Trans. Energy Conversion, Vol. 18, Issue 1, March 2003, pp. 107 – 112.
- [14] D.C. Hanselman, Brushless Permanent-Magnet Motor Design. New York: McGraw-Hill, 1994.
- [15] J.R. Hendershot and T.J. E. Miller, Design of Brushless Permanent-Magnet Motor. Oxford, U.K., Magna Physics/Clarendon, 1994.
- [16] Z. Bingyi, Z. Wei, Z. Fuyu, F. Guihong, "Design and Starting Process Analysis of Multipolar Line-Start PMSM," Proc. ICEMS 2007, Seoul, 8-11 Oct., 2007, pp. 1629-1634.
- [17] T. Miller, "Synchronization of line-start permanentmagnet AC motor," IEEE Trans. Power Apparatus and Systems, vol. PAS-103, July 1984, pp 1822-1828.
- [18] T. Miller, "Transient performance of permanent magnet AC machines," IEEE IAS Annual Meeting 198 1, Philadelphia, pp. 500-503.
- [19] A. M. Trzynadlosky, "Diagnostic of mechanical abnormalities in induction motor using instantaneous electric power," in Proc. 1997 Int. Electr. Machines Drives Conf., Milwaukee, WI, pp. 91-93.
- [20] H. A. Toliyat and S. Nandi, "Condition monitoring and fault diagnosis of electrical machines—A review," in Proc. IEEE-IAS 1999 Annu. Meeting, Phoenix, AZ, Oct. 3-7, 1999, pp. 197-204.
- [21] N. M. Elkasabgy, A. R. Eastman, and G. E. Dawson, "Detection of broken bar in the cage rotor on an induction machine," IEEE Trans. Ind. Appl., vol. 28, no. 1, pp. 165-171, Jan./Feb. 1992.
- [22] A. M. Trzynadlosky, "Diagnostic of mechanical abnormalities in induction motor using instantaneous electric power," in Proc. 1997 Int. Electr. Machines Drives Conf., Milwaukee, WI, pp. 91-93.
- [23] H. A. Toliyat and S. Nandi, "Condition monitoring and fault diagnosis of electrical machines—A review," in Proc. IEEE-IAS 1999 Annu. Meeting, Phoenix, AZ, Oct. 3-7, 1999, pp. 197-204.
- [24] N. M. Elkasabgy, A. R. Eastman, and G. E. Dawson, "Detection of broken bar in the cage rotor on an induction machine," IEEE Trans. Ind. Appl., vol. 28, no. 1, pp. 165-171, Jan./Feb. 1992.